Journal of Alloys and Compounds, 203 (1994) 1–6
JALCOM 855

Coexistence of ordered and disordered phases in a $CeGe_{2-x}$ single crystal

B. Lambert-Andron
Laboratoire de Cristallographie, CNRS, 166X, F-38042 Grenoble (France)

N. Boutarek
Laboratoire des Matériaux et du Génie Physique, ENSPG, BP 46, F-38402 St. Martin d'Hères (France)

J. Pierre
Laboratoire L. Néel, CNRS 166X, F-38042 Grenoble (France)

R. Madar
Laboratoire des Matériaux et du Génie Physique, ENSPG, BP 46, F-38402 St. Martin d'Hères (France)

(Received March 16, 1993)

Abstract

The phase diagram of the $CeGe_{2-x}$ compounds ($0.1 < x < 0.6$) is redefined. The occurrence of two tetragonal phases in equilibrium in a single crystal of $CeGe_{1.54}$ is observed by optical microscopy. The two phases are identified by X-ray diffraction as ordered and disordered variants of the $ThSi_2$ structure; their magnetic properties are characterized by neutron diffraction, magnetic and resistivity measurements.

1. Introduction

The crystal structure and physical properties of cerium intermetallic compounds of formula close to CeX_{2-x} ($X \equiv Si$, Ge) have been widely studied [1–3]. These compounds crystallize in two main structural types, tetragonal $ThSi_2$ (space group $I4_1/amd$) and $GdSi_2$ (space group *Imma*), which are closely related. The type of structure depends on the stoichiometry, the nature of the non-metal and the temperature.

For the compounds $CeGe_{2-x}$ a transition from orthorhombic to tetragonal is observed on lowering the germanium concentration, whereas the reverse occurs for $CeSi_{2-x}$. The orthorhombic phases show a selective repartition of vacancies on one of the two silicon or germanium sites of the $GdSi_2$ structure [4, 5].

In addition, various types of superstructures related to the ordering of vacancies can exist. The compound $CeGe_{1.6}$ [6] exhibits a (3a,3a) superstructure of tetragonal $ThSi_2$ with a succession of dense and vacant planes of germanium along the *c* axis.

For particular starting compositions of the melted alloy close to $CeGe_{1.75}$ we have been able to observe for a single crystal the coexistence of two tetragonal phases with epitaxial relationship. One of these two phases corresponds to the already observed (3a,3a) superstructure, while the other seems to crystallize in the $ThSi_2$ structure.

We will show in the following that crystallographic study, metallographic examination and physical properties (magnetism and resistivity) prove the thermodynamic equilibrium between these two phases.

2. *Preparation of samples*

Polycrystalline bulk samples of $CeGe_{2-x}$ were prepared with various Ge/Ce atomic ratios in the range $0.25 < x < 0.5$. Stoichiometric mixtures of cerium rods (3N) and germanium lumps (6N) were inductively melted in a cooled Hukin-type copper crucible under argon. Then the samples were ground under an argon atmosphere and annealed for 6 days at 850 °C under a high vacuum.

A single crystal was grown by the Czochralski method using a modified Hukin-type cold crucible [7]. The starting composition of the melt was $CeGe_{1.75}$. The crystal was pulled from the induction-levitated melt while a polycrystalline rod of the alloy was pushed simultaneously inside the cold crucible. The pulling rate was 3 mm h^{-1} and [001] was found to be the preferential growth direction.

This sample contains two phases. The strong lines in the X-ray diffraction pattern can be indexed in two

SSDI 0925-8388(93)00855-S

different tetragonal $ThSi_2$ structures with the lattice constants $a = 4.227$ Å, $c = 14.166$ Å and $a = 4.270$ Å, $c = 14.083$ Å respectively.

This situation has been already observed at low temperature in $CeSi_{1.86}$ [8] and $PrSi_{1.9}$ [9] and at room temperature in $CeGe_{1.2}Si_{0.475}$ [10].

The chemical composition of the single crystal was determined by microprobe analysis. The single-crystal rod was oriented by X-ray Laue diffraction. A small crystal was used for crystallographic studies and slices measuring $5 \times 1 \times 0.7$ mm^3 were cut along the [100] and [001] crystallographic axes for magnetization and resistivity measurements.

3. Variation in lattice constants in $CeGe_{2-x}$ compounds

Room temperature lattice parameters of the samples were determined by X-ray powder diffraction Seeman–Bohlin-type focusing cameras using Cr $K\alpha_1$ radiation with silicon as internal calibration standard.

Analysis of the X-ray diffraction data shows that the diffraction pattern of the studied compounds can be indexed in the $ThSi_2$ or $GdSi_2$ structure. However, in these compounds we observe weak lines in the diffraction diagram which indicate ordering effects and superstructures. In a first step these additional reflections were neglected and lattice parameters were calculated assuming the tetragonal $ThSi_2$ or orthorhombic $GdSi_2$ cell.

In the $CeGe_{2-x}$ ($0.25 < x < 0.5$) compounds three different structures could be observed: two tetragonal-type $ThSi_2$ structures (Q_1 and Q_2) and an orthorhombic-type $GdSi_2$.

The variation in the lattice parameters and lattice volume is shown in Fig. 1.

The micrograph of the single-crystal $CeGe_{1.75}$ (Fig. 2) shows two different phases. Separate analysis of each of these phases was found to be impossible, but the average composition of the sample corresponds to $CeGe_{1.52}$.

This composition is considerably different from the starting composition $CeGe_{1.75}$. This is probably due to the evaporation of germanium during the synthesis of the single crystal.

A phase transition from a tetragonal $ThSi_2$-type (high temperature) to an orthorhombic $GdSi_2$-type (low temperature) structure for the congruent compound $CeGe_{2-x}$ has been included in the most recent version of the Ce–Ge phase diagram [11]. The transition temperature has been reported to vary in the homogeneity range of the corresponding phase from 490 °C (for its equilibrium with Ge) to 560 °C (for its equilibrium with CeGe). The structural change corresponding to

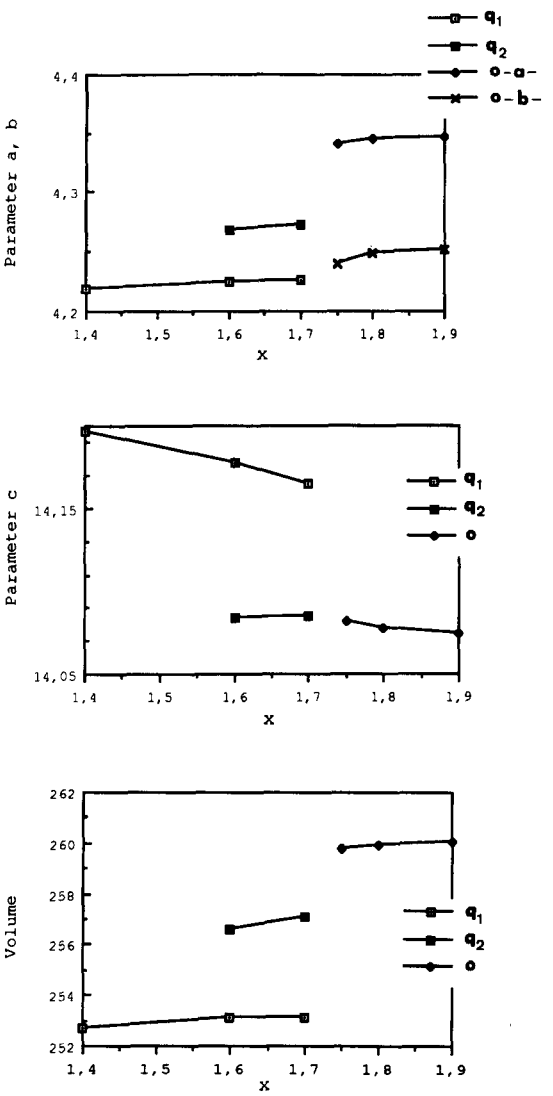

Fig. 1. Evolution of cell parameters and volume with Ge content x.

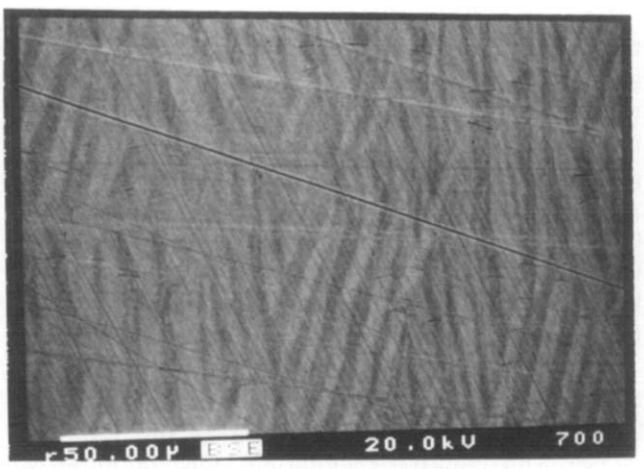

Fig. 2. Optical micrograph of $CeGe_{1.75}$ single crystal.

rather small compositional variations which has been discussed in this paragraph shows the extreme complexity of this system.

The hypothesis of a eutectic transformation of the liquid into two tetragonal phases ($L \rightarrow Q_1 + Q_2$) seems feasible. In this case the two tetragonal phases Q_1 and Q_2 are considered to melt congruently.

4. Structural investigation of the phase Q_2

The X-ray powder diffraction diagram showed two sets of reflections corresponding to the two phases Q_1 and Q_2. The phase Q_1 is like the compound $CeGe_{1.6}$ [6] with a superstructure of $ThSi_2$ ($a = 3a_t$, $c = c_t$).

X-ray diffraction experiments were carried out on an approximately spherical single crystal of Q_2 using a four-circle diffractometer. The experimental conditions are given in Table 1.

A first refinement performed in the orthorhombic group *Imma* ($GdSi_2$ type) did not show a preferential ordering of the vacancies on one of the two germanium sites. Subsequently the space group $I4_1/amd$ ($ThSi_2$ type) was chosen with disordered vacancies.

The intensities were merged (Laue symmetry) with an agreement factor of 0.06 on equivalent reflections.

Refinement by the least-squares method was performed using the SDP program [12], applying a spherical absorption correction.

The reliability factor between the observed and calculated intensities was $R = 0.08$ and $R_w = 0.10$. This rather poor value can be related to the disorder of the vacancies, the occurrence of some stacking faults and also to the approximation of a spherical shape for absorption correction.

The positional and thermal parameters are given in Table 2 and the interatomic distances in Table 3.

The high values of anisotropic thermal factors for the site occupied by germanium atoms and vacancies indicate static and/or dynamic disorder. The refinement of the scattering factor for the germanium site gives the occupancy factor $p = 0.77(2)$ and leads to the formula $CeGe_{1.54}$, in good agreement with microprobe analysis.

TABLE 1. Experimental conditions

Single-crystal size	Sphere, $R = 0.07$ mm
Diffractometer	Nicolet
Scan mode	Ω
Scan width	1.2°
Scan speed	1.5° min^{-1}
Θ limits	$3° < \Theta < 35°$
Number of independent reflections	146 ($F < 4\sigma$)

5. Magnetic properties and magnetic structures

The magnetic susceptibility was measured at low temperature on two pieces of single crystal cut along the *a* and *c* axes. The susceptibility is larger along the *c* axis and is similar to that of $CeGe_{1.6}$ [6].

At low temperature the magnetization *M* for a field *H* applied along the *c* axis is much larger than for *H* along the *a* axis (Fig. 3) and saturates for fields larger than 2 T. From the anisotropy of magnetization the system is nearly Ising like at low temperatures. The value of *M* at 1.5 K under 2 T is 1.55 μ_B, close to that of the $CeGe_{1.6}$ ferromagnet.

However, the spontaneous magnetization along *c* is only 1 μ_B and saturation is reached in a two-step process with critical fields of about 1 and 1.7 T. This behaviour suggests the coexistence of an antiferromagnetic phase in addition to the ferromagnetic one, the former undergoing metamagnetism above 1 T. It is quite straightforward to attribute the two magnetic phases to the two crystallographic phases and we verify this through neutron diffraction in the following.

Assuming that the local magnetic moment of Ce is the same in the two phases (1.55 μ_B from the saturation value), or in other words that the crystal field ground state is not very different in the two phases, we find that there is 63% of ferromagnetic and 37% of metamagnetic phase in the single crystal at 1.5 K.

In addition, the magnetization process with two nearly equal steps suggests that by increasing the field, one downward magnetic moment on one site of the metamagnetic phase is reversed, followed by the reversal of the spin on another magnetic site.

Finally, magnetic isotherms show that a change in the magnetic state occurs at about 5 K; some spontaneous magnetization (ferromagnetism) remains until 7 K, whereas the two-step magnetization process disappears.

Powder neutron diffraction experiments were performed using the multidetector diffractometer at the Siloé reactor (Nuclear Center, Grenoble). The diffraction patterns were recorded at 1.45, 5.3 and 12.5 K (Fig. 4). The incident wavelength was 2.494 Å.

The diagram at 1.45 K shows additional magnetic reflections.

(1) There is an increase in some nuclear reflections of the $I4_1/amd$ structure, *e.g.* (101), (103) and (112), which is characteristic of ferromagnetic ordering. The (004) allowed reflection is absent, hence the moment direction is confirmed to be the *c* direction.

(2) Some reflections not allowed by the space group appear, *e.g.* (110), corresponding to antiferromagnetism within the chemical cell. However, the (002) line being absent implies that for this magnetic phase too the moment lies along the *c* axis. The magnetic structure

TABLE 2. Positional and thermal parameters and their estimated standard deviations

Atom	x	y	z	B(1,1)	B(2,2)	B(3,3)	B(A2)
Ce	0.000	0.000	0.000	0.0182(6)	B(1,1)	0.00198(7)	1.40(2)
Ge	0.000	0.000	0.5821(5)	0.014(2)	0.057(4)	0.0043(3)	2.9(1)

$B(1,2)=B(1,3)=B(2,3)=0$. The form of the anisotropic displacement parameter is $\exp[-(B(1,1)\times h_2+B(2,2)\times k_2+B(3,3)\times l_2+B(1,2)\times hk+B(1,3)\times hl+B(2,3)\times kl)]$.

TABLE 3. Interatomic distances

Atoms	Distance (Å)
Ce–Ce	4.1182(2)
Ce–Ge	3.183(4)
	3.220(4)
Ge–Ge	2.446(6)
	2.316(6)

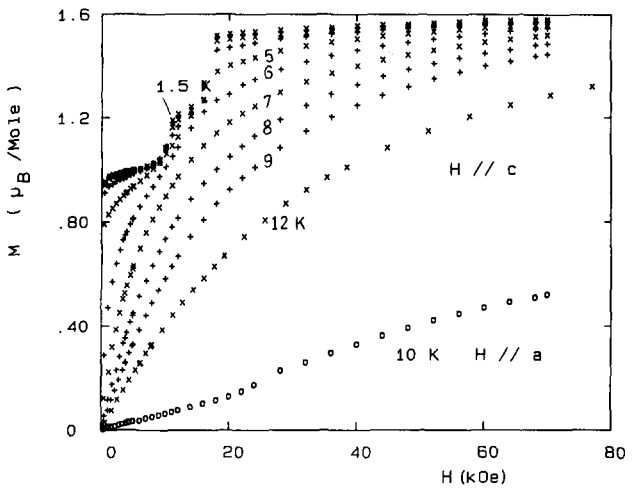

Fig. 3. Magnetization of $CeGe_{1.54}$ single crystal for a field applied along *c* or *a* direction.

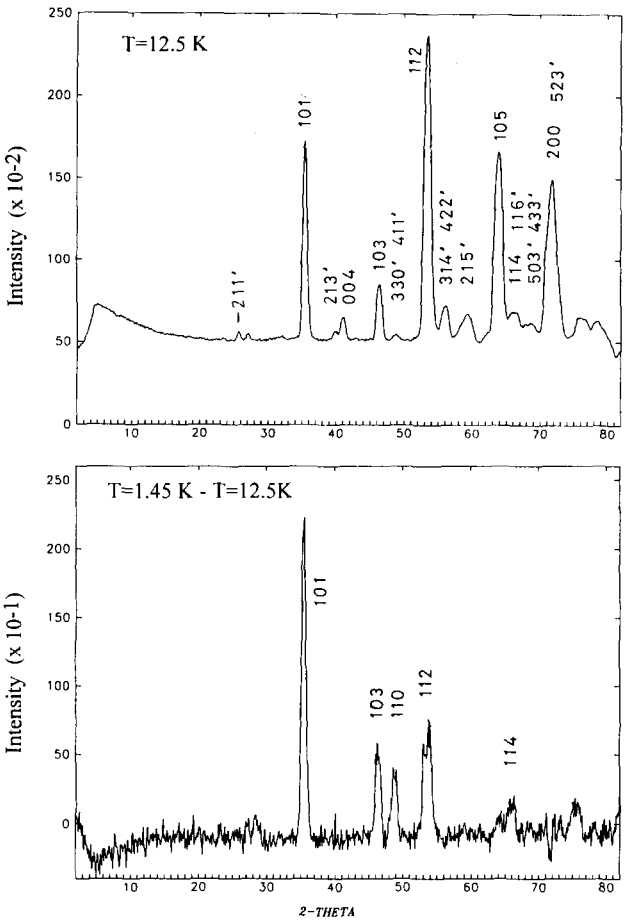

Fig. 4. Neutron diffraction pattern for $CeGe_{1.54}$ at 12.5 K and difference pattern (1.45 K−12.5 K).

may be determined without ambiguity even if only one line can be precisely measured. The four basis atoms in the tetragonal cell are described in Table 4.

The antiferromagnetic mode is + − + −, where the spins change their direction between consecutive planes along the *c* axis.

The two-step magnetization process can then be understood as a sign reversal on one of the sites, giving a + + + − mode before ferromagnetic saturation is reached.

The magnetic intensities are given in Tables 5 and 6. In order to evaluate the magnetic moment, we must either know the percentage of the two phases in the sample, which is not possible because the diffractometer resolution is not sufficient to resolve the nuclear reflections, or assume as before that the two magnetic phases have the same local moment. With this last assumption the phase percentage is obtained as 61% of ferromagnetic and 39% of antiferromagnetic phase at 1.45 K, in good agreement with magnetic measurements on the single crystal. The magnetic moment is then estimated to $1.6\pm0.1\ \mu_B$.

TABLE 4. Atomic positions for Ce atoms

Ce_1	0	0	0
Ce_2	0	$\frac{1}{2}$	$\frac{1}{4}$
Ce_3	$\frac{2}{2}$	$\frac{1}{2}$	$\frac{1}{2}$
Ce_4	$\frac{1}{2}$	0	$\frac{3}{4}$

TABLE 5. Magnetic intensities for ferromagnetic phase Q_1

$h\ k\ l$	I_{obs}	$\sigma\ (I_{obs})$	I_{calc}
0 0 2	0	5	0
1 0 1	325	32	336
0 0 4	0	5	0
1 0 3	205	20	194
1 1 2	541	100	594

$R=0.07$, $R_w=0.05$. The normalization factor is deduced from nuclear intensities at 125 K.

TABLE 6. Magnetic intensities for antiferromagnetic phase Q_2

$h\ k\ l$	I_{obs}	$\sigma\ (I_{obs})$	I_{calc}
0 0 2	0	5	0
1 1 0	232	20	232
0 0 4	0	5	0

Even if reflections cannot be resolved, there are some indications concerning the nature of the two phases. The Bragg angle for the antiferromagnetic (110) reflection is in better agreement with the lattice parameters of the disordered phase and it is logical to think that the (3a,3a) phase in this sample has the same ferromagnetic structure as that of the ferromagnetic (3a,3a) $CeGe_{1.6}$ sample [6]. The ferromagnetic reflections included in Table 5 are indexed in the $ThSi_2$ cell.

The reflection pattern at 5.3 K suffers from very poor statistics for the magnetic intensities, since the ordered moment has decreased owing to the proximity of the ordering point. It is hardly possible to say whether the antiferromagnetic (110) reflection still exists or not at this temperature.

6. Resistivity

The temperature dependence of the resistivity has also been measured on two pieces of single crystal cut along the c and a axes. Measurements were done by the four-probe a.c. method.

The shape of the resistivity is similar along the two axes (Fig. 5). A large drop in resistivity occurs at the Curie point of 7 K. A change in concavity near 40 K can be explained by crystal field effects. Figure 5(b) represents the resistivity derivative for $I \| c$. In addition to a lambda-type anomaly at 7 K, we notice a strong peak near 4.5 K. This peak points to a change in magnetic structure at this temperature. From the large magnitude of this anomaly, corresponding to a large disorder entropy, it is probable that this temperature corresponds to the Néel temperature of the antiferromagnetic phase.

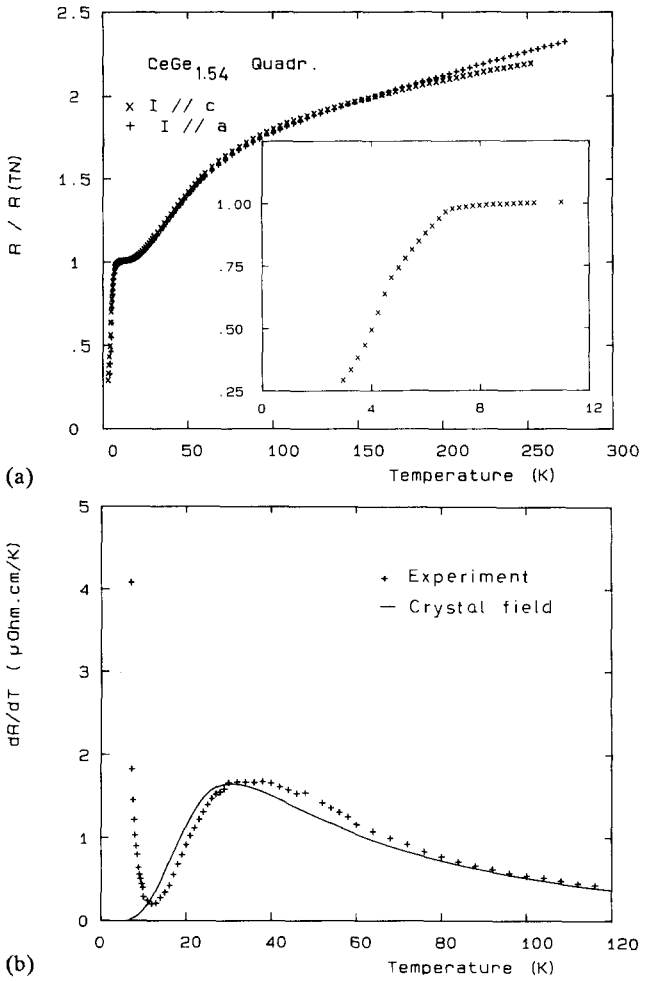

Fig. 5. (a) Resistivity of $CeGe_{1.54}$ single crystal along a and c axes. (b) Resistivity derivative dR/dT compared with crystal field fit (continuous curve) in paramagnetic range.

In the paramagnetic range the maximum at 35 K is analogous to Schottky anomalies for specific heat. It corresponds to the increase in spin disorder scattering due to the thermal population of crystal field excited levels. The description of such an anomaly is possible using *e.g.* the theory of Van Peski-Tinbergen and Dekker [13] as long as the crystal field parameters are known. Using parameters determined by neutron inelastic scattering and anisotropy data for $CeGe_{1.6}$ [6], we obtain a fit (continuous curve in Fig. 5(b)) in fair agreement with experiment, indicating that the crystal field indeed does not change too much in this range of composition or with the order of Ge atoms.

7. Discussion

The complex phase diagram of $CeGe_{2-x}$ compounds ($0.1 < x < 0.6$) was redefined and the existence of two

tetragonal phases and one orthorhombic phase was shown. The occurrence of two tetragonal phases in equilibrium in a $CeGe_{1.54}$ single crystal is note worthy, the composition of each phase being very similar.

Vacancies were found to be ordered in the phase Q_1, while they are disordered (no long-range order) in the phase Q_2. Neutron diffraction experiments at low temperature show the persistence of the two phases Q_1 and Q_2 with two different magnetic structures.

This mixture of phases may arise either directly from coprecipitation from the liquid or from phase separation in the solid state.

Some of the observed features lead to favouring the first hypothesis.

(1) The optical micrographs (Fig. 2) are very similar to the patterns of oriented eutectics.

(2) The grains all have the same orientation towards the crystal growth axis.

(3) The onset of large cracks in the more constricted phase shows an important differential dilatation, therefore the structure was established well above room temperature.

(4) No crystallographic transformation was detected by high temperature susceptibility measurements.

It is unusual to find in a single crystal the coexistence of two phases in epitaxial relationship, with very close compositions and respectively ordered and disordered crystallographic structures based on the same basic structure. The origin of this phenomenon is not yet clearly understood.

Acknowledgment

We thank P. Arons of the Neutron Diffraction Group of Grenoble Nuclear Center for helping us during the neutron diffraction experiments.

References

1 I. Mayer and Y. Eshdat, *Inorg. Chem., 7* (1968) 1904.
2 E. Houssay, A. Rouault, O. Thomas, R. Madar and J.P. Senateur, *Appl. Surf. Sci., 38* (1989) 156.
3 E.I. Gladyshevski, *Crystal Chemistry of Silicides and Germanides, Metallurgya, Moscow, 1971.*
4 P. Schobinger-Papamantellos, T. Jassen, D.B. Mooij and K.H.J. Buschow, *J. Less-Common Met., 162* (1990) 197.
5 S. Auffret, J. Pierre, B. Lambert Andron, R. Madar, E. Houssay, D. Schmitt and E. Siaud, *Physica B, 173* (1991) 265.
6 B. Lambert Andron, E. Houssay, R. Madar, F. Hippert, J. Pierre and S. Auffret, *J. Less-Common Met., 167* (1990) 53.
7 O. Thomas, J.P. Sénateur, R. Madar, O. Laborde and E. Rosencher, *Solid State Commun., 55* (1985) 629.
8 R. Madar, B. Lambert, E. Houssay, C. Meneau d'Anterroches, J. Pierre, O. Laborde, J.L. Soubeyroux, A. Rouault, J. Pelissier and J.P. Sénateur, *J. Mater. Res., 5* (1990) 2126.
9 B. Lambert, F. Sayetat, S. Auffret, J. Pierre and R. Madar, *J. Phys.: Condens. Matter, 3* (1991) 3113.
10 N. Boutarek, R. Madar, B. Lambert Andron, S. Auffret and J. Pierre, *J. Alloys Comp., 189* (1992) 9.
11 V.N. Eremenko, Yu.I. Buyanov and V.G. Batalin, *Phase Diagrams of Binary Systems of Germanium with Rare Earth Metals,* 1975, *Fiz. Khim. Kondensir. Faz.*, Kiev, Russian Federation, p. 191.
12 B.A. Frenz, SDP *Program*, College Station, TX, 1985.
13 T. Van Peski-Tinbergen and A.J. Dekker, *Physica, 29* (1963) 917.